Time course of motion adaptation: Motion-onset visual evoked potentials and subjective estimates

Michael Hoffmann [a,b], Thorsten J. Dorn [a], Michael Bach [a,*]

[a] *Elektrophysiologisches Labor, Universitäts-Augenklinik, Killianstraße 5, D-79106 Freiburg, Germany*
[b] *Institut für Biologie I (Zoologie), Universität Freiburg, Hauptstraße 1, D-79104 Freiburg, Germany*

Abstract

The aim of this study was to quantitatively describe the dynamics of adaptation to visual motion with electrophysiological and psychophysical methods in man. We recorded visual evoked potentials (VEPs) to motion onset of random dot patterns from occipital and occipito-temporal electrodes during a succession of adaptation-recovery sequences. In these sequences the test stimulus was used to set the adaptation level: seven trials with 70% motion duty cycle (adaptation) followed by seven trials of 7% motion duty cycle (recovery). In a similar paradigm we determined the length of the perceptual motion after-effect to obtain a psychophysical measure of the time course of motion adaptation. Our results show a highly significant reduction of the N2 amplitude in the maximally compared to the minimally adapted condition ($P < 0.001$). Electrophysiological and psychophysical results both indicate that adaptation to visual motion is faster than recovery: The data were fit with an exponential model yielding adaptation and recovery time constants, respectively, of 2.5 and 10.2 s for the N2 amplitude (occipito temporal derivation) and of 7.7 and 16.7 s for the perceptual motion after-effect. Implications for the design of motion stimuli are discussed, e.g. a motion stimulus moving 10% of the time may lead to about 30% motion adaptation. © 1998 Elsevier Science Ltd. All rights reserved.

Keywords: Cortex; Human; Motion; Adaptation; VEP

1. Introduction

It is well known that perception of visual motion in humans is very susceptible to adaptation: After prolonged viewing of visual motion this property appears psychophysically as a deterioration of performance in motion detection tasks such as direction discrimination, speed discrimination, and velocity estimation and the perception of illusory motion (Taylor, 1963; Keck & Pentz, 1977; Müller & Greenlee, 1994). The latter is known as the motion after-effect (MAE; reviewed by Wade, 1994). This adaptability of motion perception can be used for both the identification and the investigation of motion processing mechanisms.

One tool to study the neural bases of motion perception in man is the motion-onset VEP (MacKay & Rietveld, 1968; Clarke 1972, 1973a,b, 1974; Tyler & Kaitz 1977; Dagnelie 1986; Göpfert, Müller & Simon, 1990). Visual motion onset evokes a potential which consists of a positivity (P1, around 100–130 ms) and a negativity (N2, around 150–200 ms) at occipital and occipito temporal electrodes. Studies on the velocity and contrast dependence, and on the origin of these components, identified N2 as motion specific whereas P1 is more likely to be associated with pattern processing (Müller & Göpfert 1988; Markwardt, Göpfert & Müller 1988; Kubovà, Kuba, Hubàcek & Vit, 1990; Schlykowa, van Dijk & Ehrenstein, 1993; Probst, Plendel, Paulus, Wist & Scherg, 1993; Kubovà, Kuba, Spekreijse & Blakemore, 1995; Bach & Ullrich 1997). Moreover, N2 matches human motion perception in its susceptibility to motion adaptation (Göpfert, Müller, Markwardt & Schlykowa, 1983; Göpfert, Müller & Hartwig, 1984; Müller, Göpfert & Hartwig, 1985; Schlykowa, van Dijk & Ehrenstein, 1993; Bach & Ullrich, 1994; Wist, Gross & Niedeggen, 1994). In contrast, the P1 amplitude even increases with adaptation, suggesting that it reflects a mechanism that is uncovered when motion mechanisms are adapted.

---

* Corresponding author. Fax: +49 761 2704060; e-mail: bach@uni-freiburg.de.

Given the high susceptibility of motion perception and especially of the motion VEP to adaptation, it seems desirable to quantitatively describe its time course. We conducted one experiment to measure the motion adaptation and recovery time constants of the VEP components evoked by motion onset and a second experiment to measure the time constants psychophysically. A preliminary account of this work has been presented previously (Dorn, Hoffmann & Bach, 1997).

2. Methods

2.1. Subjects

VEPs were recorded from 11 human observers with normal or corrected to normal visual acuity (≥ 0.9). They gave their informed consent to participate in the experiment. Eight of these were naive as to the experimental question.

2.2. Stimuli

Stimuli were generated by a computer (Power Macintosh 8500) and presented on a CRT with a frame rate of 120 Hz at a viewing distance of 57 cm. The stimulus pattern consisted of random dots (pattern size $19 \times 19°$; mean luminance 26 cd/m²; contrast 98%; element size $0.1 \times 0.1°$; 50% black and 50% white elements). A stationary fixation target (size: $1.5 \times 1.5°$) was in the center of the pattern. The pattern was surrounded by a grey mask (size: $29 \times 22°$; mean luminance 26 cd/m²). We used two test stimuli differing only in their motion duty cycle (time of motion/full cycle time). A motion sequence consisted of an abrupt onset of continuous motion at 5.7°/s for either 233 or 2333 ms followed by a stationary phase for 3100 or 1000 ms, respectively. Hence the motion duty cycle was either 7% or 70%.

2.3. Procedure

The test stimuli themselves set the adaptation level, based on the results from pilot experiments that the unknown time constants were not less than 1 s and not higher than 60 s. The adaptation level was modified by alternating adaptation and recovery periods by the use of two different motion duty cycles: seven adaptation stimuli (70% duty cycle) were followed by seven recovery stimuli (7% duty cycle). This cycle, consisting of 14 stimuli (total duration: 46.6 s), was presented 15 times in each of ten blocks. Averaging across blocks yielded 14 motion-onset VEPs, seven of them sampling the adaptation period and the remaining seven sampling the recovery period. The first two adaptation and recovery cycles of each block were discarded to allow the system to reach a stable state. One session lasted about 3 h.

2.4. VEP Recording

VEPs were recorded from three derivations, Oz-Fpz, Otl (5 cm left from Oz) and Otr (5 cm right from Oz) versus linked ears. The ground electrode was attached to the right wrist. Signals were amplified, filtered (0.3 Hz-70 Hz, Toennies Physiological Amplifier), and digitized at a sampling rate of 500 Hz. Trials were analyzed off line over the interval from 100 ms before to 500 ms after motion onset. Trials with blinks, detected with a threshold criterion of 100 µV, were discarded, leaving 76 to 120 sweeps per stimulus for each observer. Averaged sweeps were digitally filtered (0–40 Hz). Baseline was defined as the mean value from -100 to $+70$ ms of the averaged trace and used as zero reference for peak measurements.

2.5. Psychophysical measurement of the adaptation and recovery time course

To determine the time course of motion adaptation and recovery psychophysically, we measured the duration of the MAE for ten of the observers who had participated in the electrophysiological experiment. We used the same stimuli as in the electrophysiological experiment. Different adaptation levels of the observers were obtained by presenting a truncated adaptation-recovery sequence; i.e. only the first one, or the first two, etc. stimuli were shown in a sequence, up to a full 14-stimulus sequence. The last stimulus of a given sequence was indicated by a beep, signaling the subject to judge the MAE (if any) after that stimulus. Test stimulus for the determination of the MAE was a stationary random dot pattern. We took the time from motion offset of the last stimulus to the moment when the observers indicated that the MAE had ceased, as a measure for the 'strength' of motion adaptation. To minimize overspill of adaptation from trial to trial there was a pause of 10 s after the observer's response before the next trial started. We determined MAE durations for each of the 14 different adaptation levels as a mean of six responses of each observer. Sequences for the different adaptation levels were presented in a randomized order. Occasionally the observers forgot to press the response button; these trials generated clear outliers in MAE duration and were discarded. The data were collected in two sessions for each observer. Three subjects reported no after-effect at all, and we excluded their data from further analysis. Hence the result of only seven subjects was used to describe the time course of the perceptual MAE. Data were normalized for each observer by taking the minimal and the maximal MAE duration as 0 and 100%, respectively.

2.6. Computational model

To quantitatively describe the time course of adaptation and recovery of the motion-onset potentials and motion perception, we interpreted the data in terms of a computational model. This model assumes that adaptation and recovery show an exponential time course and that the time constants for adaptation and recovery are independent. By fitting this model to the data (means of all observers) we obtained time constants for adaptation and recovery. The effect of any adaptation or recovery epoch depends on the adaptation state at the start of the respective epoch. The latter, in turn, depends on the entire previous history of adaptation/recovery epochs. This can be expressed in a case-switching difference equation. A closed integration, while analytically possible, yields unwieldly expressions. So we integrated the model numerically using a time step of $\Delta t = 5$ ms. The model has two free parameters, the adaptation time constant (τ_{ada}) and the recovery time constant (τ_{rec}).

$$\Phi_{t + \Delta t} = \begin{cases} \Phi_t + \left((1 - \Phi_t) \dfrac{\Delta t}{\tau_{ada}} \right) & |\text{in the adaptation interval} \\[2mm] \Phi_t - \left(\Phi_t \dfrac{\Delta t}{\tau_{rec}} \right) & |\text{in the recovery interval} \end{cases}$$

$$(1)$$

The internal adaptation state Φ, a hypothetical construct, was mapped to VEP amplitude assuming linearity and introducing the maximal (A_{max}) and minimal (A_{min}) absolute VEP amplitude as further free parameters:

$$A_{VEP} = A_{min} + (A_{max} - A_{min}) \cdot (1 - \Phi) \qquad (2)$$

To relate the internal adaptation state Φ to the psychophysical data (MAE duration) we introduced the perception threshold (s) of the MAE as a free parameter:

$$s = \Phi \cdot e^{-t_{MAE}/\tau_{rec}} \qquad (3)$$

This equation has the following rationale: We assume that at termination of the adapting sequence, the subject's internal adaptation state decays exponentially with τ_{rec}. As long as this adaptation state exceeds some threshold s, the subject perceives the MAE. Eq. (3) can be resolved for t_{MAE}

$$t_{MAE} = -\tau_{rec} \ln (s/\Phi) \qquad (4)$$

The subjects' perceptual MAE-duration times had been normalized by subtracting the minimal duration and dividing by the maximal value. These normalization constants can be calculated from the model and do not need to enter as further free parameters.

The model parameters were estimated by minimizing χ^2 with the curve-fit function of Igor (WaveMetrics), which is based on the Levenberg-Marquardt algorithm. For the calculation of the standard errors of the time constants for the electrophysiological data, the standard errors of the data cannot be used, since they are, due to interindividual variation, widely overestimated and normalization of the data is difficult. In order to address this problem, we calculated the deviation of the data from the fit and refed it into the error propagation of the fit program to get an error estimate of the time constants. It has to be noted that these standard errors thus express the deviation of the data from the model, disregarding the error of the actual data.

3. Results

Grand mean responses across 11 subjects are depicted in Fig. 1. The adaptation epoch is shaded. Potentials are shown for the Oz versus Fz and the Ot* versus linked ears derivation. The Ot* derivation was introduced for the following rationale: Motion onset potentials can be strongly lateralized. This lateralization is stable within subjects but variable among subjects, i.e. some subjects have more pronounced potentials at Otr others at Otl (Andreassi & Juszczak 1982). In order to maximize N2 amplitudes we evaluated the dominant Ot derivation, i.e. with maximal N2 amplitudes, of each subject for the grand mean of Ot*.

Over the course of adaptation N2 amplitudes decrease while P1 amplitudes increase. Over the course of recovery the reverse effect is observed. Fig. 2A, B display the time courses (mean ± SEM) of the components P1 and N2 for both electrode positions. OT*-N2 amplitudes were compared for the minimal and maximal adaptation condition (arrows in Fig. 2B). The amplitude difference was found to be highly significant (paired *t*-Test: $P < 0.001$).

3.1. Adaptation and recovery time constants

The N2 amplitudes in Fig. 2A, B —as determined from the grand mean data—were fit with the exponential model (continuous curves). The resulting time constants show that N2 adaptation ($\tau_{ada} = 5.2 \pm 0.7$ s and 2.5 ± 0.2 s at Oz and Ot*, respectively) is faster than N2 recovery ($\tau_{rec} = 34 \pm 15.6$ s and 10.2 ± 1.2 s at Oz and Ot*, respectively). The SEMs indicate that the Ot* fit is much better than the Oz fit. The perceptual motion adaptation was measured by determining the length of the MAE. Normalized data were fitted with an exponential model, taking into account that the
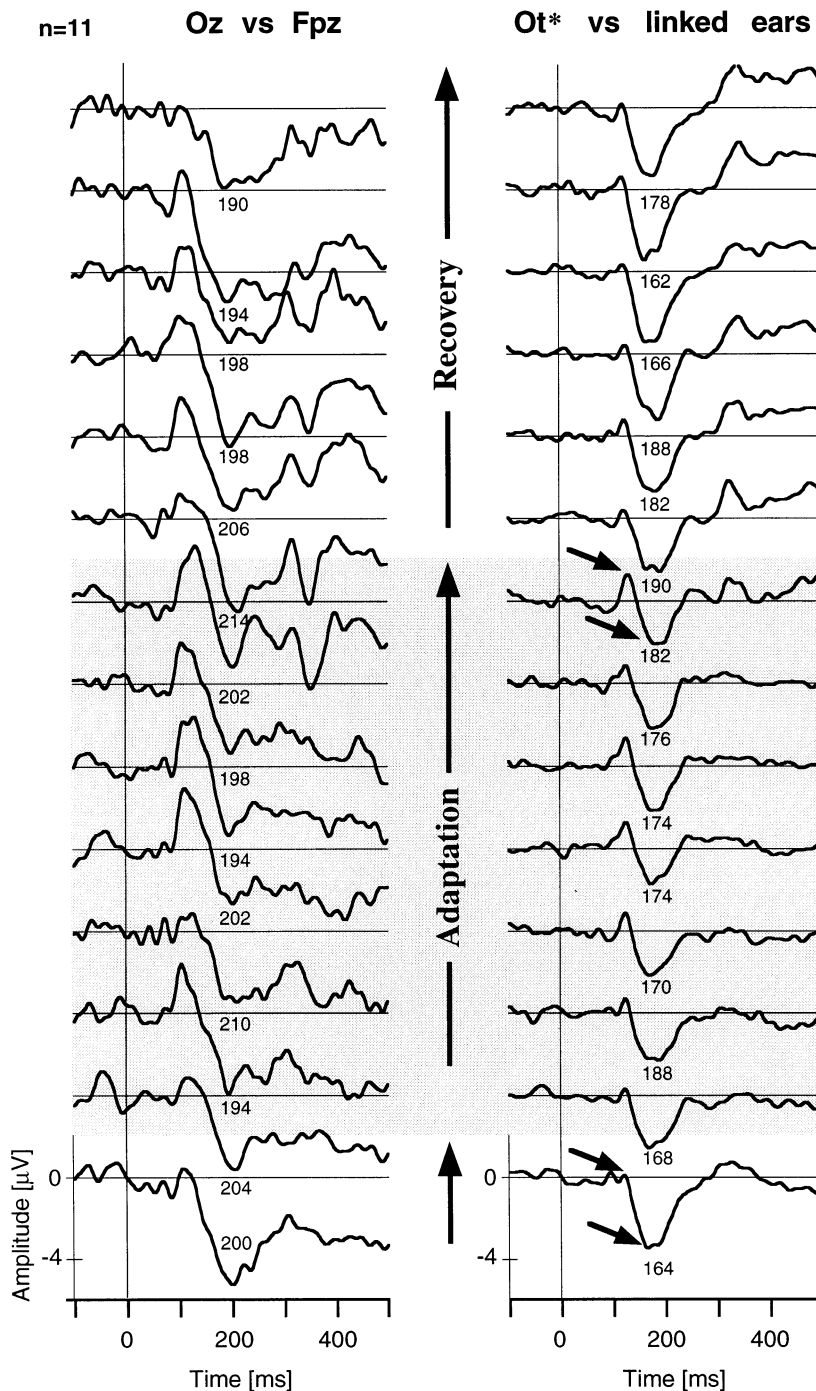
Fig. 1. Grand mean potentials of 11 subjects during the adaptation–recovery sequence for two electrode positions. For the Ot* derivation each subject's dominant side was included in the grand mean. Vertical lines indicate motion onset. During adaptation (the seven bottom traces) and recovery (the top traces) motion lasted for 2333 and 233 ms, respectively. Shaded area indicates VEPs during the adaptation period. Note that the VEP represents the adaptation state at the start of the stimulus, which was set by the preceding stimulus. The numbers next to the traces represent the latency of N2 in ms. The adaptation-recovery sequence modulates the P1 and N2 amplitudes in opposite directions. For example: with least adaptation (bottom) N2 is large and P1 small; with maximal adaptation (top of shaded area) P1 is large and N2 reduced. The arrows point at the maximally and minimally adapted P1 and N2.

duration of the after-effect had to be transformed with the inverse exponential function to yield the adaptation level on an internal scale (Fig. 2C). The time constants are 7.7 ± 5.2 s and 16.7 ± 4.6 s for adaptation and recovery, respectively, the threshold was estimated as $15 \pm 6\%$ of the internal adaptation state.
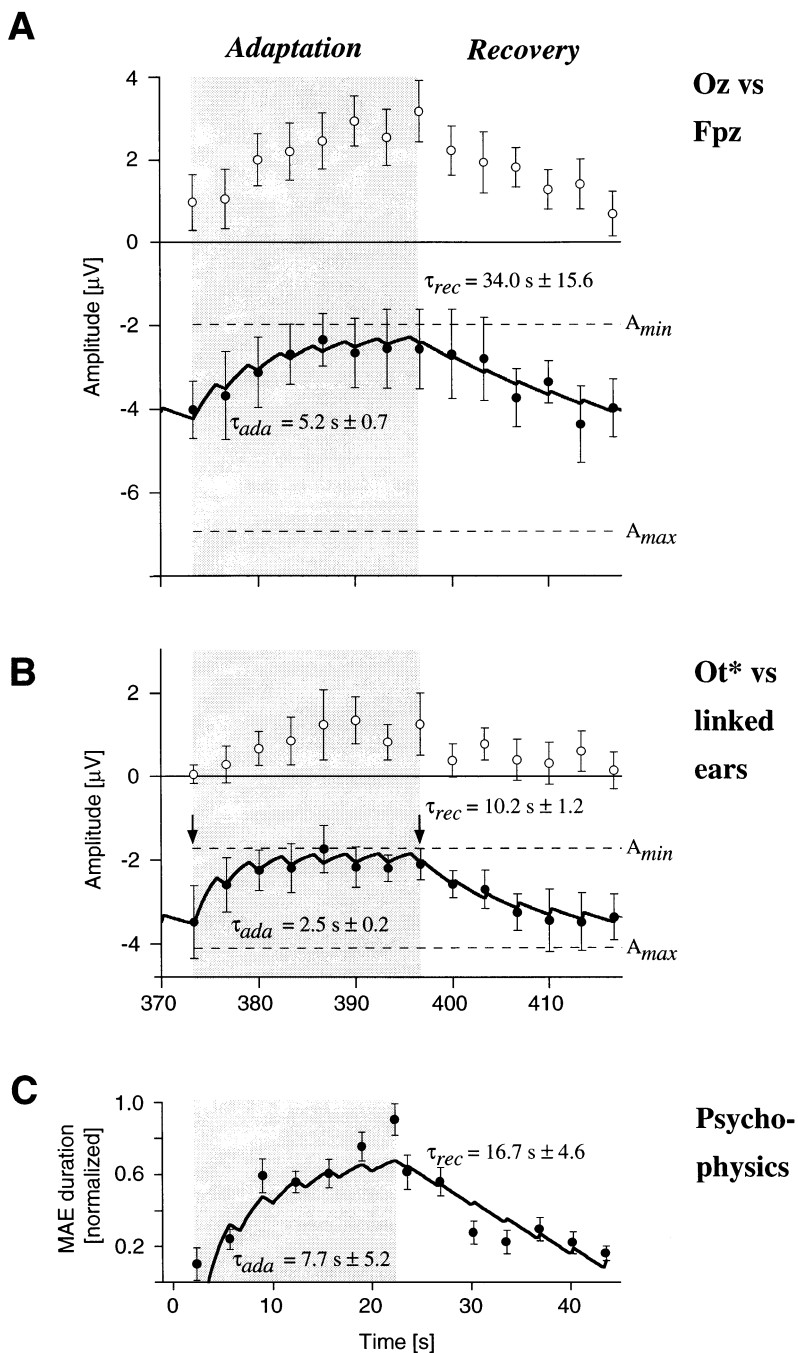
Fig. 2. Electrophysiological (grand mean amplitudes) and psychophysical data during the adaptation–recovery sequence ± SEM and the fit of the exponential model (solid line). P1 (empty symbols) and N2 amplitudes (filled symbols) and MAE durations clearly vary during the adaptation-recovery sequence. P1 and N2 have an inverse relationship (note the different polarity). The N2 amplitudes for the minimal and maximal adaptation condition at OT* (arrows in B) differ highly significantly (paired t-test: $P < 0.001$). Time constants ± SEM for the fits are indicated. SEMs of the N2-time constants depend on the goodness of the fit (see text). A and B: P1 and N2 amplitudes of the grand mean data shown in Fig. 1. Time axis is given for the fit, absolute times are not relevant for the grand mean data, since the design was cyclic. A_{max} and A_{min} (see Eq. (2)) are -6.93 ± 1.6 and -2.0 ± 0.14 at Oz and -4.1 ± 0.1 and -1.7 ± 0.05 at OT*, respectively. (C) Mean MAE durations of seven observers, normalized (0 = minimal individual MAE duration, 1 = maximal individual MAE duration). The fit (C, right part) has not the typical shape of an exponential function: The internal adaptation state is assumed to have an exponential time course. The MAE duration, however, is not directly related to this internal adaptation state. It is itself a function of the exponential decay of the MAE. This is taken into account for the fit as described in methods, which entails the untypical shape of the exponential fit.

4. Discussion

4.1. Adaptation and recovery time constants of N2 and the perceptual motion after-effect

As expected, the motion-onset VEP changed markedly during the adaptation-recovery sequence. The variation of N2 could be predicted with a computational model that quantitatively describes the time course of adaptation and recovery with the respective time constants. Most reliable time constants for adaptation and recovery of the N2 data were obtained for Ot*, 2.5 ± 0.2 s and 10.2 ± 1.2 s, respectively. Though they do not match exactly, they are consistent within the error margin with those obtained in our psychophysical measurement of motion adaptation and recovery, 7.7 ± 5.2 s and 16.7 ± 14.6 s, respectively.

Previously Giaschi, Douglas, Marlin and Cynader (1993) obtained time constants of motion adaptation and recovery from single cell studies in the cat in area 17. They found small time constants (5–19 s) and for simple cells additional direction dependent long time constants (1.5–2.5 min), which they attributed to contrast and motion adaptation, respectively. Tootell, Reppas, Dale and Look (1995) measured time constants not for adaptation, but for recovery from motion adaptation psychophysically and with fMRI in human cortical area MT, obtaining 9.2 and 8.3 s, respectively. We find time constants in the range of seconds for adaptation and recovery, which is in agreement with the work of Tootell, Reppas, Dale and Look (1995) and with the short time constants of Giaschi, Douglas, Marlin and Cynader (1993). Unlike the latter we attribute the short time constants as determined from the perceptual MAE to motion adaptation, since the perceptual MAE is clearly due to direction selective mechanisms.

We interpret the finding of asymmetric time constants as follows: If motion adaptation is viewed in terms of 'fatigue' (Barlow & Hill 1963), it is quite likely that resource depletion and reconstitution are different processes which need not necessarily have identical time course. However, we tend to view motion adaptation in terms of active gain adjustment mechanisms, like in contrast adaptation (Greenlee & Heitger 1988). For instance, Carandini and Ferster (1997) have shown in intracellular recordings that in the adapted state the visual input is not reduced, but that a superimposed tonic hyperpolarization leads to reduced spike activity. The details of these mechanisms are unknown, but again it appears quite plausible that adaptation and recovery may have different time constants.

The similarity of the electrophysiological and psychophysical time constants for motion adaptation and recovery suggests that both arise from the same processes. However, a note of caution has to be added to this interpretation: Psychophysical motion adapta-tion has been shown to be confined to the direction of the adaptation stimulus (Raymond 1993), whereas the adaptation of the N2 component of the motion-onset VEP is not completely direction specific (Bach, Hoffmann & Ullrich 1996). This could mean that N2 reflects not only motion processing, but also non-direction specific processing, e.g. flicker detection.

4.2. Practical implications of the N2-adaptation dynamics

Any motion VEP experiment should take adaptation to the test stimulus into account. Our quantitative data on N2[1]'s adaptation dynamics may help to effectively design future paradigms, especially if similar stimulus patterns are used. We simulated data for different duty cycles (Fig. 3): For five duty cycles we calculated the time course of the adaptation level using the electrophysiological fit parameters. As is shown in Fig. 3A, it takes about six cycles, i.e. 20 s, to reach a steady adaptational state for each of the five duty cycles. Furthermore, for any duty cycle we calculated the asymptotic adaptation level that is reached after many adaptation/recovery epochs (Fig. 3B). To calculate the asymptotic adaptation level as a function of duty cycle, we used an analytical solution to the model. This solution leads to iterative formulas which take the form of a geometric progression:

$$\Phi\infty_{\text{end of motion epoch}} = \frac{1 - m}{1 - m \cdot s}$$

$$\Phi\infty_{\text{end of stationary epoch}} = \frac{(1 - m) \cdot s}{1 - m \cdot s} \tag{5}$$

where the symbols

$$m = e^{\frac{t_{\text{moving}}}{\tau_{\text{ada}}}} \quad \text{and} \quad s = e^{\frac{t_{\text{stationary}}}{\tau_{\text{rec}}}} \tag{6}$$

were introduced for simplicity. Unlike the simpler model by Bach and Ullrich (1994), which assumed equal time constants for adaptation and recovery, adaptation depth here is not linearly related to duty cycle. The strongest effects occur for short duty cycles: A duty cycle of 10% leads to an adaptation of about 30% estimated electrophysiologically, or 20% estimated psychophysically. These figures assume the validity of the duty cycle model.

There are, however, two caveats: (1) Our pilot studies showed that the time between two motion onsets, i.e. the total duration of the trials, is an additional parameter that influences the adaptation level to some degree. This might be attributed to adaptation due to the mere motion onset. The shorter the trials are, the more this parameter will contribute. (2) The duty cycle model
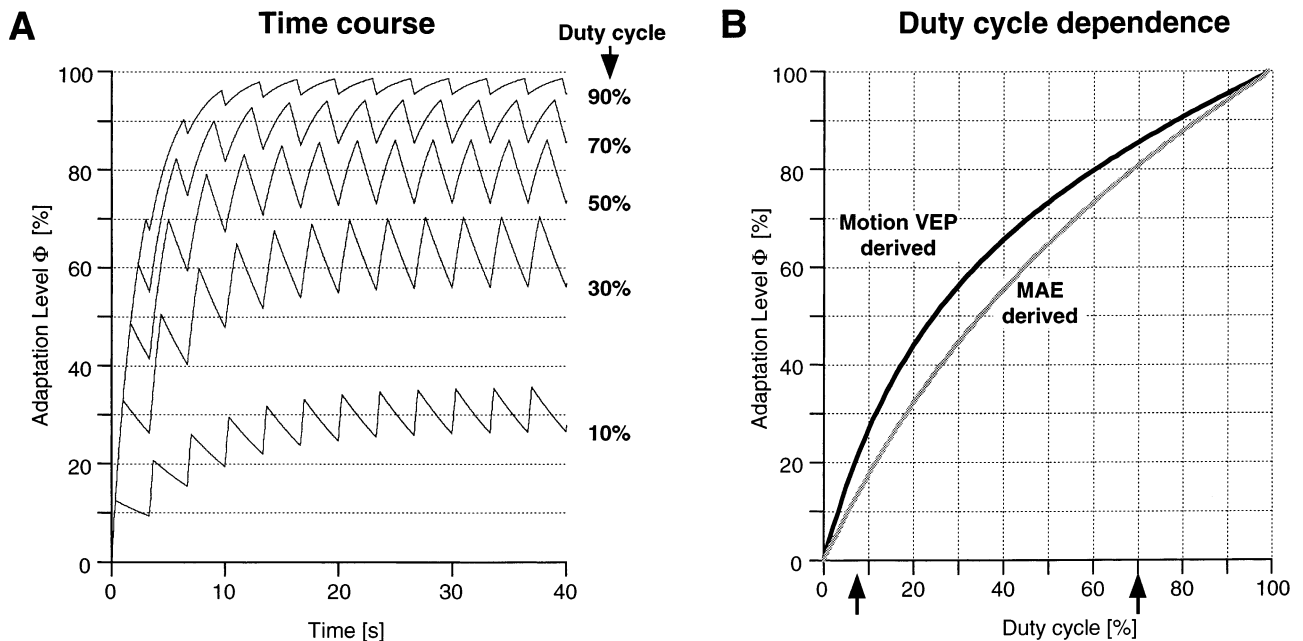
Fig. 3. Effect of duty cycle on the internal adaptation state Φ calculated with the time constants of N2 at Ot* and the perceptual after-effect for a stimulus duration of 3.333 s based on the exponential model (see text). (A) Time course of adaptation for five different duty cycles. The saw-tooth shape of the traces arises from the alternation of motion and stationarity, i.e. adaptation and recovery periods. After about six trials the adaptation level settles to a steady state around two asymptotic values. (B) Dependence of asymptotical adaptation level $\Phi\infty$ on duty cycle. The motion VEP derived adaptation level is estimated from the N2 amplitudes. The MAE derived adaptation level is given for the internal adaptation level scale and not for the MAE durations. Arrows indicate duty cycles used in this investigation. A duty cycle of 10% entails already 20–30% adaptation.

holds only for stimulus durations shorter than the time constants. Therefore the given duty cycle-adaptation level pairs apply quantitatively only to conditions in which the trials have a full cycle duration similar to the one used in these experiments (around 3 s).

Furthermore our data show that the amplitude difference P1-N2 is not a useful measure for the adaptational state of the motion system, since both P1 and N2 covaried inversely, which leaves their difference little affected during the adaptation-recovery sequence.

Electrophysiological (N2 amplitude) and perceptual motion adaptation (MAE duration) show a similar time course: Time constants are in the range of seconds and adaptation is faster than recovery (by about a factor 3)

Acknowledgements

References

Andreassi, J. L., & Juszczak, N. M. (1982). Hemispheric sex differences in response to apparently moving stimuli as indicated by visual evoked potentials. *International Journal of Neuroscience, 17,* 83–91.

Bach, M., & Ullrich, D. (1994). Motion adaptation governs the shape of motion-evoked cortical potentials. *Vision Research, 34,* 1541–1547.

Bach, M., Hoffmann, M., & Ullrich, D. (1996). Motion-onset VEP: missing direction-specificity of adaptation? *Investigative Ophthalmology and visual Science* (*Supplement*), *37,* 2040.

Bach, M., & Ullrich, D. (1997). Contrast dependence of motion-onset and pattern-reversal VEPs: Interaction of stimulus type, recording site and response component. *Vision Research, 37,* 1845–1849.

Barlow, H. B., & Hill, R. N. (1963). Evidence for a physiological explanation of the waterfall phenomenon and figural after-effects. *Nature, 200,* 1345–1347.

Carandini, M., & Ferster, D. (1997). A tonic hyperpolarization underlying contrast adaptation in cat visual cortex. *Science, 276,* 949–952.

Clarke, P. G. H. (1972). Visual evoked potentials to sudden reversals of the motion of a pattern. *Brain Research, 36,* 453–458.

Clarke, P. G. H. (1973a). Visual evoked potentials to changes in the motion of a patterned field. *Experimental Brain Research, 18,* 145–155.

Clarke, P. G. H. (1973b). Comparison of visual evoked potentials to stationary and moving patterns. *Experimental Brain Research, 18,* 156–164.

Clarke, P. G. H. (1974). Are visual evoked potentials to motion reversal produced by direction-sensitive brain mechanisms? *Vision Research, 14,* 1281–1284.

Dagnelie, G. (1986). Pattern and motion processing in primate visual cortex. A study in visually evoked potentials. Thesis, Amsterdam.

Dorn, T. J., Hoffmann, M., & Bach, M. (1997). Motion adaptation time constants of the motion-onset VEP. *Investigative Ophthalmology and visual Science* (*Supplement*), *38,* 4608.

Greenlee, M. W., & Heitger, F. (1988). The functional role of contrast adaptation. *Vision Research*, *28*, 791–797.

Giaschi, D., Douglas, R., Marlin, S., & Cynader, M. S. (1993). The time course of direction selective adaptation in simple and complex cells in cat striate cortex. *Journal of Neurophysiology*, *70*, 2024–2034.

Göpfert, E., Müller, R., Markwardt, F., & Schlykowa, L. (1983). Visuell evozierte Potentiale bei Musterbewegung. *Zeitschrift für EEG und EMG*, *14*, 47–51.

Göpfert, E., Müller, R., & Hartwig, M. (1984). Effects of movement adapation on movement-visual evoked potentials. *Documenta Ophthalmologica Proceedings Series*, *40*, 321–324.

Göpfert, E., Müller, R., & Simon, E.-M. (1990). The human motion onset VEP as a function of stimulation area for foveal and peripheral vision. *Documenta Ophthalmologica*, *75*, 165–173.

Keck, M. J., & Pentz, B. (1977). Recovery from adaptation to moving gratings. *Perception*, *6*, 719–725.

Kubová, Z., Kuba, M., Hubàcek, J., & Vìt, F. (1990). Properties of visual evoked potentials to onset of movement on a television screen. *Documenta Ophthalmologica*, *75*, 67–72.

Kubová, Z., Kuba, M., Spekreijse, H., & Blakemore, C. (1995). Contrast dependence of motion-onset and pattern-reversal evoked potentials. *Vision Research*, *35*, 197–205.

MacKay, D. M., & Rietveld, W. J. (1968). Electroencephalogram potentials evoked by accelerated visual motion. *Nature*, *217*, 677–678.

Markwardt, F., Göpfert, E., & Müller, R. (1988). Influence of velocity, temporal frequency and initial phase position of grating patterns on motion VEP. *Biomedica Biochimica Acta*, *47*, 753–760.

Müller, R., & Göpfert, E. (1988). The influence of grating contrast on the human cortical potential visually evoked by motion. *Acta Neurobiologica Experientia*, *48*, 239–249.

Müller, R., Göpfert, E., & Hartwig, M. (1985). VEP-Untersuchungen zur Kodierung der Geschwindigkeit bewegter Streifenmuster im Kortex des Menschen. *Zeitschrift für EEG und EMG*, *16*, 75–80.

Müller, R., & Greenlee, M. W. (1994). Effect of contrast and adaptation on the perception of the direction and speed of drifting gratings. *Vision Research*, *34*, 2071–2092.

Probst, T., Plendel, H., Paulus, W., Wist, E. R., & Scherg, M. (1993). Identification of the visual motion area (area V5) in the human brain by dipole source analysis. *Experimental Brain Research*, *93*, 345–351.

Raymond, J. E. (1993). Movement direction analysers: Independence and bandwidth. *Vision Research*, *33*, 767–775.

Schlykowa, L., van Dijk, B. W., & Ehrenstein, W. H. (1993). Motion-onset visual-evoked potentials as a function of retinal eccentricity in man. *Cognitive Brain Research*, *1*, 169–174.

Taylor, M. M. (1963). Tracking the decay of the after-effect of seen rotary motion. *Perceptual and Motor Skills*, *16*, 119–129.

Tootell, R. B. H., Reppas, J. B., Dale, A. M., & Look, R. B. (1995). Visual motion after-effect in human cortical area MT revealed by functional magnetic resonance imaging. *Nature*, *375*, 139–141.

Tyler, C. W., & Kaitz, M. (1977). Movement adaptation in the visual evoked response. *Experimental Brain Research*, *27*, 203–209.

Wade, N. J. (1994). A selective history of the study of visual motion after-effects. *Perception*, *23*, 1111–1134.

Wist, E. R., Gross, J. D., & Niedeggen, M. (1994). Motion after-effects with random-dot chequerboard kinematograms, relation between psychophysical and VEP measures. *Perception*, *23*, 1155–1162.